8
Nanostructured Materials for Selective Collection of Trace-Level Metals from Aqueous Systems

Sean A. Fontenot, Timothy G. Carter, Darren W. Johnson, R. Shane Addleman, Marvin G. Warner, Wassana Yantasee, Cynthia L. Warner, Glen E. Fryxell, and John T. Bays

8.1
Introduction

Several separations and filtration techniques are available for the collection of trace-level species and each method must be matched to a specific application. For trace-level metals in solution arguably the best and most widely used methods involve solid phase sorbent materials that provide effective capture of desired metal species. Effectiveness of the solid phase sorbent for any given application is determined by availability, cost, and performance. Activated carbon and ion exchangers are widely available and relatively cheap but lack, in most cases, the performance necessary for many analytical applications. Activated carbon and ion exchangers generally fail to have the selectivity and affinity needed for trace analyte collection from actual environmental matrices.

To understand and respond to situations involving toxic materials it is critical to quickly identify the toxic material(s) involved and the extent of contamination. This is a key issue for circumstances ranging from responding to terrorist attacks to monitoring the effects of environmental remediation. Unfortunately, analytical technology does not presently exist to meet these needs. Instruments powerful enough to meet the required speed, sensitivity, and selectivity requirements often do not function well outside of rigorously controlled laboratory conditions and are usually very complex and expensive. Simple screening methods that provide immediate results in the field enable on-site, near real-time decisions. These field screening methods are typically less costly and more rapid than formal laboratory analysis; this is significant since site testing and monitoring typically involves extensive sampling. To meet this need, a wide range of field screening methods for identifying chemical, biological, and nuclear materials is presently being marketed and used. Unfortunately, existing field assay methods are typically inadequate because they lack the selectivity and sensitivity needed to provide reliable information. The degree and type of improvement needed vary with the application but sensitivity improvements of greater than 1000× are typically required, and much larger enhancements would usually be preferred. This large

Trace Analysis with Nanomaterials. Edited by David T. Pierce and Julia Xiaojun Zhao

ISBN: 978-3-527-32350-0

leap in analytical performance is very unlikely to be achieved with incremental improvements in measurement procedure, instrument design, or improved electronics. A new analytical approach is required.

In many circumstances the deficiencies in selectivity and sensitivity could be addressed with high-performance sorbent materials that selectively concentrate target analytes. In addition to concentrating target analytes the sorbent can exclude interfering species and provide a uniform, well-defined sample matrix for analysis. Sorbents coupled with instrumentation could be used for either real-time analysis of the signature species or as a rapid screening method to flag those samples that require more detailed analysis. Sorbents coupled with rugged, compact instrumentation could provide portable, yet highly sensitive, field analyzers that could be quickly reconfigured for new analytes simply by changing the sorbent material. Sorbents used in these systems could be designed to be reusable, renewable, or disposable depending upon the instrument configuration desired and material chemistries involved. These same sorbents could be used to improve the performance of traditional laboratory techniques with more effective sample clean up.

This chapter is a discussion and review of various advanced nanostructured materials applicable to the selective collection of trace-level analytes from aqueous systems for sensing and separation applications. For consistency and comparison, when possible, materials expressing thiol surface chemistry are used as examples. While a plethora of surface chemistries exist, and many have relevance to environmental challenges, thiol surface chemistry is highly effective for the capture of many toxic heavy metals from aqueous systems, and serves as a useful baseline to compare materials performance. Further, thiol surface chemistry has been demonstrated on a range of nanostructures and therefore provides continuity and a common platform for nanomaterial comparison. This chapter is organized into sections by material type. Discussions are broken down into the materials science and application of:

- functionalized nanoporous silica material;
- functionalized magnetic nanomaterials;
- carbon-based nanostructured materials;
- other materials such as zeolites, and imprinted polymers;
- concluding thoughts on economics and the future of nanostructured materials in trace analysis.

8.2
Sorbents for Trace-Metal Collection and Analysis: Relevant Figures of Merit

Solid-phase sorbent materials provide effective capture and preconcentration of trace-level metal species from aqueous matrices. Effective solid-phase extraction (SPE) sorbents allow separation for remediation purposes, but they are also ideal for analytical applications since preconcentration of analytes prior to assay

separates the analyte(s) from the sample matrix and concentrates them into a smaller volume prior to measurement. Once preconcentration is complete, the analyte can be stripped from the SPE material by an appropriate method (e.g., via acid, thermalization, etc.) and then quantified by analysis. Alternatively, the SPE material can be assayed directly for some applications [1]. This allows one to improve the sensitivity, selectivity, and speed of an analytical process.

Sorbents may be evaluated in terms of affinity and capacity for target species as well as how quickly they can extract target species (kinetics). Most of the sorbents discussed here consist of support materials having surfaces functionalized with organic metal-binding groups. The surface chemistry of the SPE material dictates the binding affinity of the material for a given analyte, and adjusting the surface chemistry of the SPE material allows it to be applied to different classes of analytes or function in different matrices. Capacity is a function of the number of binding units on the sorbent, which, in turn, depends on the surface area of the support and the degree of functionalization. Kinetics depend mostly on mass transport through the sorbent material and the extent to which the material may be dispersed in the sample matrix.

Binding affinities of sorbents are typically expressed using the distribution coefficient (K_d); K_d, (ml g^{-1}) is simply a mass-weighted partition coefficient between the solid phase and liquid supernatant phase as represented in Equation (8.1):

$$K_d = \frac{(C_O - C_f)}{C_f} \times \frac{V}{M} \tag{8.1}$$

where

C_o and C_f are the initial and final concentrations, respectively, in the solution of the target species,
V is the solution volume in ml,
M is the mass of the sorbent.

The V/M term is simply the liquid to solid (L/S) ratio of the sample solution to the sorbent. In other words, V/M is the ratio of the volume of sample analyzed to the amount of sorbent used and provides a measure of the amount of sorbent needed for a given analysis. The higher the K_d, the more effective the sorbent material is at capturing and holding the target species. In practical terms, a sorbent with a high K_d for a given target will allow uptake of the target even at very low concentrations. In general, K_ds of ~10^3 ml g^{-1} are considered good and those above 10^4 ml g^{-1} are outstanding [2].

For applications involving trace analysis, capacity is less important than affinity since saturation of the sorbent is typically not an issue and the amount of analyte extracted by the SPE material is limited by the magnitude of the analyte distribution coefficient (K_d). By employing high surface area, dispersible, and specifically functionalized sorbents one can drive the interaction of the sorbents with the analytes in the sample, effectively facilitating both separation and preconcentration. The remainder of this chapter uses K_d as the figure of merit for demonstrating analyte selectivity.

8.3
Thiol-Functionalized Ordered Mesoporous Silica for Heavy Metal Collection

Removal of heavy metals, such as mercury (Hg), lead (Pb), thallium (Tl), cadmium (Cd), and arsenic (As), from natural waters has attracted considerable attention because of environmental contamination and their adverse effects on environmental and human health. Introduction of sorbent functionalities into nanoporous structures has significantly improved the performance of those sorbent materials in metal removal when compared to conventional sorbent beds [3–5]. This section reviews the ability of thiol-functionalized ordered mesoporous silica, termed thiol self-assembled monolayer on a mesoporous support (SH-SAMMS™), to capture heavy metals. This material is superior to commercial sorbents, such as Duolite® GT-73 resins, and Darco® KB-B activated carbon. SH-SAMMS also presents new uses beyond environmental applications. These include chelation therapies and biomonitoring of heavy metals.

8.3.1
Performance Comparisons of Sorption Materials for Environmental Samples

The ability of a sorbent material to capture a metal ion depends on the pK_a of its primary ligating functional group, the stability constant of the metal–ligand complex, the presence of competitive ligands in solution, the pH of the solution [6], and the metal ion's capacity to undergo hydrolysis [7]. Figure 8.1 shows the binding affinity (K_d) of SH-SAMMS to various metal ions in HNO_3 spiked filtered river water. As anticipated from Pearson's hard-soft acid-base theory (HSAB) [8], soft ligands like thiol groups prefer to bind soft metals like Hg and Ag, rather than a relatively harder metal such as Co. Based on the K_ds, SH-SAMMS is an outstanding sorbent for Hg, Ag, Pb, Cu, and Cd ($K_d > 50\,000\,ml\,g^{-1}$) and a good sorbent for As in river water at neutral pH. SH-SAMMS could effectively bind Hg, Ag, and As for the entire pH range (pH 0 to 8.5), Cu from pH 2 to 8.5, and Cd and Pb from 6 to 8.5. Work in our laboratory reveals that Hg is strongly bound to SH-SAMMS even in acid concentrations as high as 5 M (HCl and HNO_3). Above pH 7, a noticeable drop in K_d of Ag, Hg, Cd, and Pb (all still above 10^5) may be a result of strong association between the metal ions and native anions in the water (e.g., between Ag^+ and reduced sulfur groups [9] or Ag^+ and $Hg^{2+}$and chloride anions [10, 11]).

Ionic strength can also vary in most pH-adjusted samples (e.g., pH 0–8.5) and may affect the metal binding affinity of a sorbent. Table 8.1 shows that ionic strength does not significantly affect the SH-SAMMS material until the concentration reaches 1 M sodium (as acetate) concentration. In the three natural waters, the affinity of SH-SAMMS for all metals tested remained virtually unaffected.

Table 8.2 summarizes K_d of metal ions from filtered groundwater (pH 6.8–6.9), measured for different sorbents. Note that thallium was added into the solutions as Tl^+ and arsenic as As^{3+}. In terms of K_d, SH-SAMMS was significantly superior to the commercial GT-73 and activated carbon (Darco KB-B) for capturing Hg, Cd,

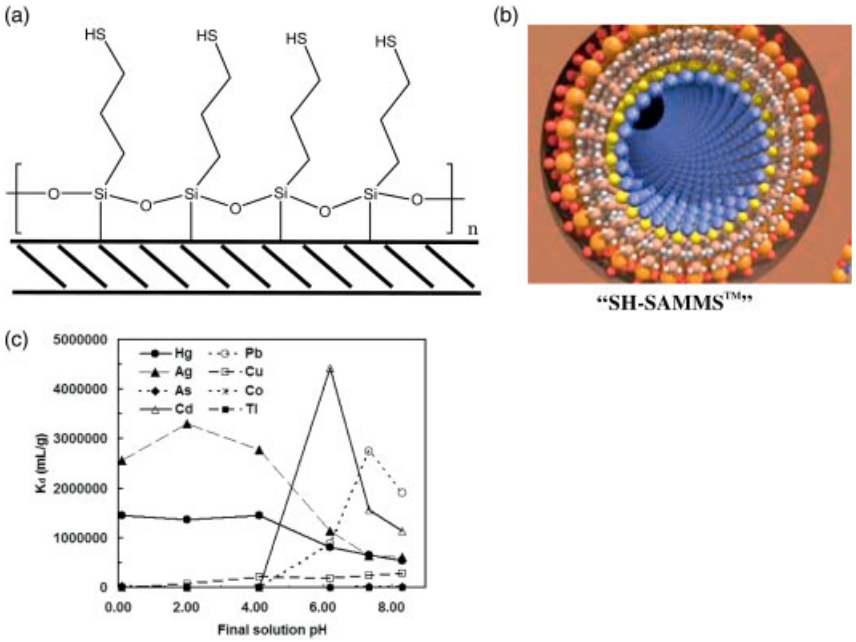

Figure 8.1 Diagram of SH-SAMMS showing a propylthiol monolayer (a) and the monolayer-lined pores (b); (c) effect of pH on the K_d of SH-SAMMS, measured in HNO_3 spiked filtered river water with a liquid to solid (L/S) ratio of 5000:1.

Table 8.1 Matrix effect on K_d (ml g^{-1}) of various metals extracted by SH-SAMMS.[a] Data reprinted with permission from Reference [12]. Copyright 2008 Elsevier.

Matrix	pH	Cu	As	Ag	Cd	Hg	Pb
Columbia River water, WA[b]	7.66	9.5×10^5	7.2×10^4	7.1×10^6	1.0×10^7	3.6×10^5	5.3×10^6
Hanford groundwater, WA[b]	8.00	1.3×10^6	5.7×10^4	1.1×10^7	1.1×10^7	5.9×10^5	5.6×10^6
Sequim Bay sea water, WA[b]	7.74	1.3×10^6	9.2×10^4	7.5×10^6	1.5×10^7	2.5×10^6	3.4×10^6
0.001 M CH_3COONa	7.14	–	4900	–	1.5×10^6	3.8×10^5	3.1×10^5
0.01 M CH_3COONa	7.19	–	2900	–	3.3×10^6	3.0×10^5	8.5×10^5
0.1 M CH_3COONa	7.21	–	4100	–	3.9×10^6	6.6×10^5	6.6×10^5
1.0 M CH_3COONa	7.28	–	2000	–	7.5×10^5	5.7×10^5	9.2×10^4

a) Reported as average value of three replicates, L/S of 5000 ml g^{-1}.
b) 0.45 micron filtered.

Table 8.2 K_d (ml g^{-1}) of metal ions extracted by selected sorbents from Hanford groundwater. [a]Data reprinted with permission from Reference [13]. Copyright 2007 American Chemical Society.

Sorbent	Final pH	Co	Cu	As	Ag	Cd	Hg	Tl	Pb
DMSA-Fe_3O_4	6.91	3000	2.7×10^5	5400	3.6×10^6	1.0×10^4	9.2×10^4	1.4×10^4	2.3×10^6
Fe_3O_4	6.93	1600	7400	5800	1.3×10^4	2400	1.6×10^4	4000	7.8×10^4
SH-SAMMS	6.80	430	1.7×10^6	950	6.7×10^7	6.6×10^4	1.1×10^6	1.5×10^4	3.5×10^5
Thiol resin[b]	6.76	890	6300	1200	1.6×10^4	1500	1.0×10^4	2200	4.1×10^4
Activated carbon[c]	6.90	790	2.6×10^4	750	2.7×10^4	1300	3.1×10^4	21	1.9×10^5

a) Reported as average value of three replicates, L/S = 10 000 ml g^{-1}, in 0.45 micron filtered groundwater.
b) GT-173 by Rohm & Hoss.
c) Darco KB-B.

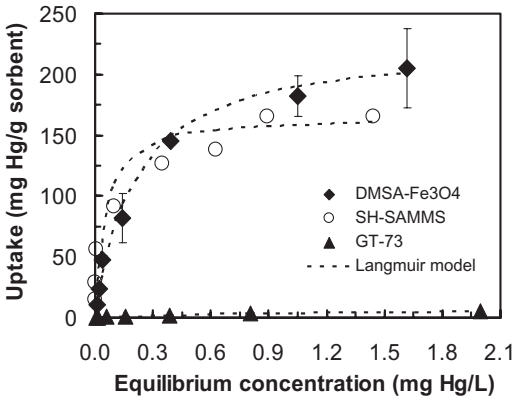

Figure 8.2 Adsorption isotherm of Hg in groundwater (pH 8.1) on DMSA-Fe_3O_4 (L/S, 5×10^5), SH-SAMMS (L/S, 5×10^5), and GT-73 (L/S, 7000); dashed lines represent Langmuir modeling of the data. Reprinted with permission from Reference [13]. Copyright 2007 The American Chemical Society.

Ag, Pb, and Tl. The superior affinity results from the multidentate chelation ability and the suitable substrate of SH-SAMMS, characteristics that are not found in the commercial resins.

Figure 8.2 shows the adsorption isotherms of Hg on SH-SAMMS, DMSA-Fe_3O_4, and GT-73 in filtered groundwater (pH 8.1) [13]. The isotherm curves present Hg uptake as a function of the equilibrium Hg solution concentration at room temperature. The saturation adsorption capacity of Hg on SH-SAMMS was found to be 167 mg g^{-1} in filtered groundwater (pH 8.1) while that of GT-73 was only 8 mg g^{-1} in the same matrix. In acidified river water (pH 1.99) a Hg adsorption capacity of 400 mg g^{-1} of SH-SAMMS has been achieved. The large surface areas

of the DMSA-Fe_3O_4 (114 $m^2 g^{-1}$, see Section 8.4 for more details) and SH-SAMMS (740–680 $m^2 g^{-1}$) afforded a high number of ligand sites on these materials, leading to large ion loading capacities. Although the capacity of GT-73 for Hg in DI water (pH 4–6) was previously reported to be 600 mg g^{-1} [14], the measured Hg capacity in groundwater reported in the highlighted study was only 8 mg g^{-1}, which suggests very poor selectivity of the GT-73's binding sites in groundwater.

In addition to covalently linking functional head-groups to mesoporous silica, an alternative connective approach utilizes weak interactions through π–π stacking between an "anchored" aromatic monolayer and chemisorbed functionalized ligands. One example studied various mono and bis-functionalized mercaptomethyl benzenes adsorbed onto mesoporous silica that had been prepared with a covalently attached phenyl monolayer (phenyl-SAMMS) [15]. Comparisons between these materials and SH-SAMMS show similar uptake capacities and kinetics. For instance, K_d values for phenyl-SAMMS chemisorbed with 1,4-bis (mercaptomethyl)benzene show similar capture levels with the covalently attached SH-SAMMS in Hanford well water matrix spiked with 500 ppb Hg^{2+}, Pb^{2+}, Cd^{2+}, and Ag^{+} ions. Therefore, the metal affinity levels of the chemisorbed phenyl-SAMMS are near equal to that of the covalently bound SH-SAMMS. Because of the weak yet stable interaction imparted by the π–π stacking, these materials have shown the ability to be stripped of their metal-loaded ligands by simple organic washes, thus leading to possible regeneration of the base phenyl-SAMMS material. The ability to regenerate sorbents is an attractive feature for both water purification and preconcentration-based technologies. Regeneration of the base material with a simple infield wash can greatly reduce the overall usage cost; an essential criterion for sorbent materials.

In addition to sorption affinity, capacity, and selectivity to the target metal ions, it is important that a sorbent material offer rapid sorption to minimize the contact time required for removal metal ions. Figure 8.3 shows the uptake rate of Pb on various sorbent materials measured in filtered groundwater (pH 7.7). Lead could be captured by SH-SAMMS at a much faster rate than the two commercial sorbents, Chelex-100 (an EDTA-based resin) and GT-73 (a thiol functionalized resin). Specifically, after one minute of contact time, over 99 wt.% of 1 mg l^{-1} of Pb was removed by SH-SAMMS, while only 48 wt.% and 9 wt.% of Pb were removed using Chelex-100 and GT-73, respectively. It took over 10 min for Chelex-100 and 2 h for GT-73 to remove over 96% of Pb [14]. GT-73 and Chelex-100 are synthesized by attaching chelating ligands to porous polymer resins, which dominate their physical properties. Thus GT-73 and Chelex-100 are subject to solvent swelling and have dendritic porosities. The SH-SAMMS has a rigid silica support and open pore structure that allow for rapid diffusion of analytes into the binding sites, resulting in extremely fast sorption kinetics.

8.3.2
Performance Comparisons of Sorption Materials for Biological Samples

Sorbents that can capture heavy metals in biological media such as blood, gastrointestinal fluids, and urine are highly desirable for several reasons. In addition

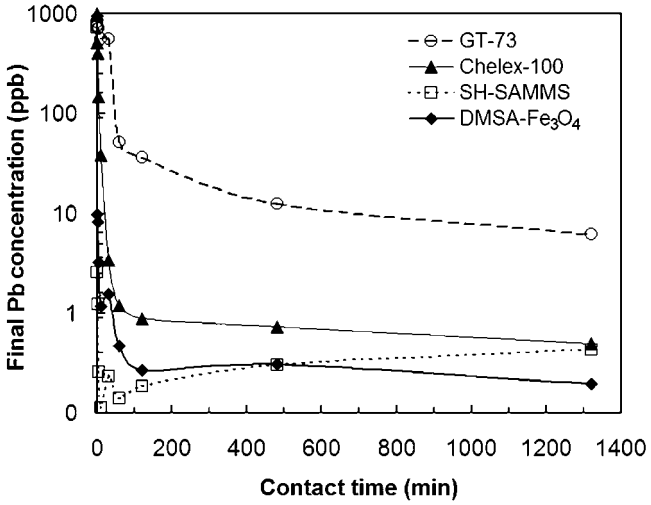

Figure 8.3 Kinetics of adsorption of 1000 ppb of Pb in filtered groundwater, pH 7.77, all with L/S of 1000, except DMSA-Fe_3O_4 with L/S of 2000. Reprinted with permission from Reference [13]. Copyright 2007 American Chemical Society.

to enhanced detection (discussed in Section 8.2), the decorporation of toxic metals from blood and gastric intestinal fluids is anticipated to provide a breakthrough in chelation therapy.

Since the 1940s, *in vivo* toxic metal immobilization has involved the use of intravenous ethylenediamine-tetraacetate (EDTA) treatment and oral or intravenous dimercaptosuccinic acid (DMSA) treatment following metal exposures. Solid sorbents are potentially better than their liquid counterparts because, as oral drugs, they can minimize the gut absorption of ingested chemicals harmful to the human body. In addition, when used in or hemoperfusion devices, they can remove the chemicals in blood that have been absorbed systemically from all routes of exposure (oral, dermal, and inhalation). This decreases the burden on the kidneys for clearing the toxic metal-bound liquid chelating agents.

SH-SAMMS captures a large percentage (~90%) of As, Cd, Hg, and a moderate percentage of Pb, presented in human urine and blood at relevant exposure levels ($50\,\mu g\,l^{-1}$). Not only can SH-SAMMS remove inorganic Hg^{2+} (Table 8.3) but it can also remove methyl Hg^{2+} (CH_3Hg^+, which is a much more problematic form of Hg); for example, at L/S of 200, 87% of methyl Hg^{2+} was removed from human plasma containing $100\,\mu g\,l^{-1}$ of the analyte. Figure 8.4 also shows the K_d of the four metals on SH-SAMMS measured in synthetic gastrointestinal fluids [16], with a pH similar to what might be encountered within the various regions of the gastrointestinal tract (pH 1–3 in stomach, pH 5.5–7 in large intestine, pH 6–6.5 in duodenum, and pH 7–8 in jejunum and ileum) [17].

In addition to their use in chelation therapies, sorbent materials that can effectively preconcentrate heavy metals from complex matrices like blood and urine

Table 8.3 Percent removal[a] of heavy metals from biological matrices using SH-SAMMS.

Matrix	L/S (ml g^{-1})	Initial metal concentration ($\mu g\,L^{-1}$)	As (%)	Cd (%)	Hg (%)	Pb (%)
Human blood	1000	50	90	93	92	15
Human urine	1000	50	93	87	89	33

a) Reported as average values of three replicates, SD < 5%.

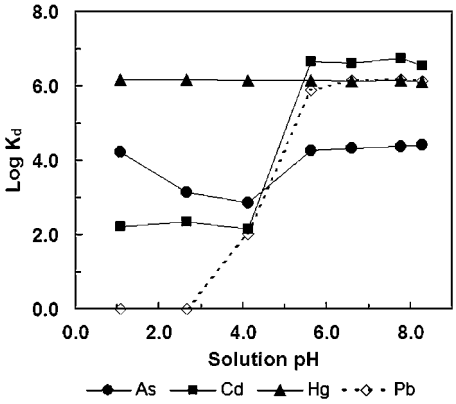

Figure 8.4 K_d of As, Cd, Hg, and Pb, measured on SH-SAMMS in synthetic gastrointestinal fluids prepared by adjusting synthetic gastric fluid (contained 0.03 M NaCl, 0.085 M HCl, pH 1.11) with 0.2 M $NaHCO_3$ to the desired pH; initial metal ion concentrations of 50 $\mu g\,L^{-1}$ and L/S of 5000.

will substantially improve biomonitoring of exposure to these species. Direct preconcentration of toxic metals from biological samples without prior acid digestion has been a challenging task for two main reasons. The proteins and macromolecules in complex biological samples can compete with the sorbent materials for binding metal ions, resulting in low capture extent (e.g., Pb example in Table 8.3). Additionally, these biomolecules tend to foul sensors, resulting in rapid degradation in response. This is especially evident with electrochemical sensors where proteins adsorb on electrode surfaces and form an insulating layer. By employing Nafion as an antifouling layer and SH-SAMMS as the metal preconcentrator, we have successfully used a SH-SAMMS-Nafion composite in electrochemical sensors for low ppb ($\mu g\,l^{-1}$) detection of heavy metals (e.g., Cd and Pb) in urine without sample pretreatment or protein fouling [12]. The resulting sensor offers detection limits similar to state-of-the-art ICP-MS methods but, unlike ICP-MS, the sensor is portable and will facilitate rapid biomonitoring of exposure to toxic metals. SH-SAMMS nanomaterials have recently emerged as

highly effective sensors for trace metal detection. Their high efficacy for metal concentration has led to their exploration to enhance a range of analytical methods, including ICP-MS, radiological measurements, and X-ray fluorescence.

8.4 Surface-Functionalized Magnetic Nanoparticles for Heavy Metal Capture and Detection

Recently, the use of functionalized superparamagnetic nanoparticles in environmentally relevant applications such as selective capture and preconcentration of specific analytes from complex samples for sensitive detection has been reported in an increasingly large number of publications and reviews [13, 18–33]. In this section we focus on the application of engineered magnetic nanoparticles (diameter < 100 nm in most cases) that contain a thiol surface functionality for the purpose of separating and detecting a wide variety of analytes from complex environmental matrices.

Preconcentration is an ideal application for functionalized magnetic nanoparticles since they provide a controllable sorbent material for solid-phase extraction (SPE). Once dispersed in solution they can rapidly contact high volumes of the sample matrix, selectively capture target analytes, and then can be recovered and manipulated by the application of a relatively strong (often > 1 T), but easily generated, magnetic field. It has been demonstrated that the intrinsically high surface area arising from the nanoscale dimensions of these nanomaterials and the ability to impart specific surface functionalization make them very effective for SPE [1]. The K_d values for various different SPE materials, including functionalized superparamagnetic nanoparticles, in filtered groundwater is shown above in Table 8.2.

Magnetic nanoparticles have the potential to be extremely effective SPE materials for the preconcentration, removal, and detection of environmental contaminants. The nanoparticle surface can be tailored to target a wide range of analytes in much the same manner as the SAMMS materials discussed above. This is accomplished by incorporation onto the surface small organic molecules that contain two sets of functional groups – one with an affinity toward the iron oxide surface (i.e., carboxylic acid and/or silane) and another with an affinity toward the target metal analyte of interest (i.e., thiol).

Complementing the ability to modify the surface chemistry with analyte-selective ligands, these materials demonstrate superparamagnetism that arises from their nanoscale single magnetic domain structures [25]. Superparamagnetic behavior manifests itself in nanoparticles smaller than a critical diameter that is both material and temperature dependent. Throughout this section, we predominantly address iron oxide nanoparticles with diameters ranging from ca. 5 to 20 nm, which falls within the established critical diameter for this material (ca. 15–20 nm) [25]. From a practical standpoint, a superparamagnetic nanoparticle has little to no remnant magnetization after exposure to a magnetic field and low to no coercivity (the field required to bring the magnetization to zero), meaning that

they will not magnetically agglomerate at room temperature [25]. This is significant for applications where it is desirable to have the nanoparticles well dispersed in the sample matrix and easily manipulated by an external magnetic field.

By exploiting the ability to remove the magnetic nanoparticles from solution with an external field and the ability to tailor the surface functionality of the nanoparticles through synthetic means, it is possible to both separate and detect with great sensitivity a wide range of heavy metal analytes. We focus our discussion on the attachment of small molecules for the purposes of both separating the target analyte from complex samples containing interferents and detecting them once separation is complete. In doing so we hope to demonstrate the efficacy and future potential of magnetic nanomaterials for the effective preconcentration and sensing of environmentally relevant heavy metal analytes from complex sample matrices (e.g., river, ground-, and ocean water).

Iron oxide nanoparticles are most commonly used for these applications since they can be made cheaply, in large quantities, and methods for their surface functionalization are well established [20, 23–25, 30, 34–37]. The iron oxide core can be made using various methods, depending on the desired size, dispersity, and magnetic characteristics. The surface can be further modified to contain the thiol functionality necessary for the intended application. In some cases applications may require exposure of the nanoparticles to harsh chemical environments, necessitating encasement of the nanoparticles in an inert shell, typically silica. Silica encasement of iron oxide nanoparticles is a common treatment to render the material more robust in low pH or biological environments and has the advantage of the silanol surface chemistry for silane ligand modification [38–42]. Noble metals are also used for encasement of the iron oxide core, depending on the application. For example, gold or silver encasement allows one to take advantage of both the magnetic and optical characteristics, such as plasmon resonance, of the core–shell materials when concentration and detection of the materials is desired [43–55].

In our work we have demonstrated that functionalized superparamagnetic nanoparticles can effectively disperse in aqueous environmental samples and sequester a wide variety of analytes including heavy metals [13, 33]. Specifically, we have employed thiol-modified Fe_3O_4 nanoparticles that are approximately 6 nm in diameter to remove Hg, Ag, Pb, Cd, and Tl from natural waters (i.e., river, ground-, and ocean water) [56]. Figure 8.5 illustrates the behavior of these materials.

The magnetic nanoparticles used in this study were highly dispersible in aqueous media, but were removed with relative ease by exposing the sample to a magnetic field. In this case the field strength was ca 1.2 T generated by a NdFeB rare earth magnet [13]. Using this setup the nanoparticles removed over 99 wt% of 1 mg l^{-1} Pb within 1 min of contact time and had a Hg capacity of over 227 mg g^{-1}. This capacity is nearly 30-fold larger than that of conventional resin-based sorbents [13]. To determine the efficacy of extraction of heavy metals by the magnetic nanoparticles, various measurements to determine the distribution coefficient (K_d) were made, as summarized in Table 8.2. Figure 8.6 illustrates that at near neutral pH in river water, the thiol-modified magnetic nanoparticles are outstanding

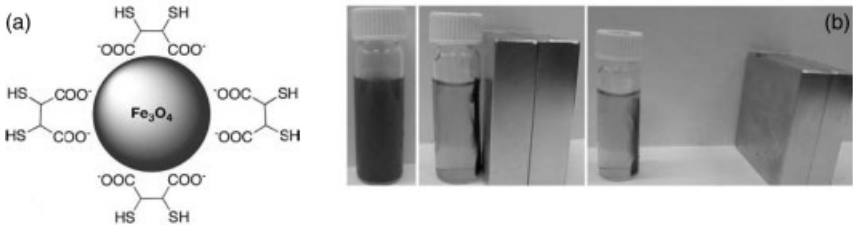

Figure 8.5 Schematic of (a) DMSA-modified Fe_3O_4 nanoparticles, and (b) removal of the nanoparticles from the liquid phase using NdFeB magnets; initial solution (left-hand panel), after 10 s with the magnet (middle panel), and when the magnet was moved to a distant position (right-hand panel). Reprinted with permission from Reference [56]. Copyright 2008 The American Chemical Society.

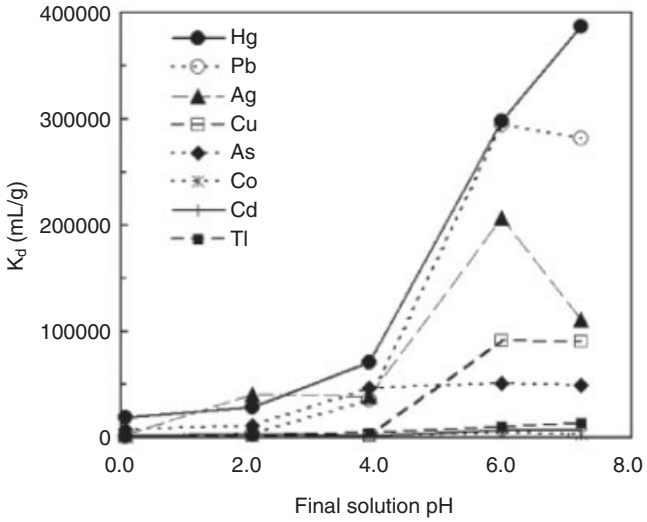

Figure 8.6 Effect of pH on K_d, measured in HNO_3 spiked unfiltered river water (L/S, 10^5:1). Reprinted with permission from Reference [13]. Copyright 2007 The American Chemical Society.

sorbent materials for soft metals such as Hg, Ag, Pb, Cu, and As ($K_d > 50\,000$). In addition, the materials were demonstrated to be a good sorbent for harder metals such as Cd, Co, and Tl [13]. Once the metals were extracted, the trace detection of the heavy metal analyte was carried out using ICP-MS after contact with the magnetic nanoparticles [13].

Materials such as magnetic nanoparticles [13] and polymer/nanoparticle composites [57–60] offer the unique capability for magnetically directed separation and sensing processes. Studies from other groups have shown similar characteristics of functionalized magnetic nanoparticles and microparticles modified with a wide

variety of affinity ligands for the extraction of heavy metals from environmental samples [61–64]. This field still remains relatively undeveloped when one is discussing the use of superparamagnetic nanoparticles between 5 and 20 nm in diameter. For instance, the behavior of nanomaterials dispersed in the environment is challenging to fully understand due to their tendencies toward aggregation and/or decomposition as well as their mobility. Many of the above reports address materials constructed from nanoparticle/polymer composites, which fall well outside of the size range of what is traditionally considered a nanomaterial (i.e., they have sizes >100 nm) [62].

Our group has demonstrated the use of both magnetic and nonmagnetic [33] high surface area sorbent materials to enhance the electrochemical detection of toxic heavy metals from natural waters [56]. Both functionalized magnetic nanoparticles and mesoporous silica were modified with a wide range of thiol-containing organic molecules that possess a high affinity toward soft heavy metals and were placed or collected at an electrode surface (Figure 8.7) [33, 56]. For instance, superparamagnetic Fe_3O_4 nanoparticles functionalized with dimercaptosuccinic acid (DMSA) were used to first bind the heavy metal contaminants from complex samples and then subsequently carry them to the surface of a magnetic electrode (Figure 8.7) [56].

By using an applied magnetic field to remove the target analytes from solution prior to electrochemical analysis, they are effectively isolated from the huge number of potential interferents present in complex sample matrixes. Using this system we have successfully overcome, at least to some extent, two of the biggest problems that prevent widespread adoption of electrochemical sensors for the analysis of metal ions in biological samples: (i) the binding of the target metals to

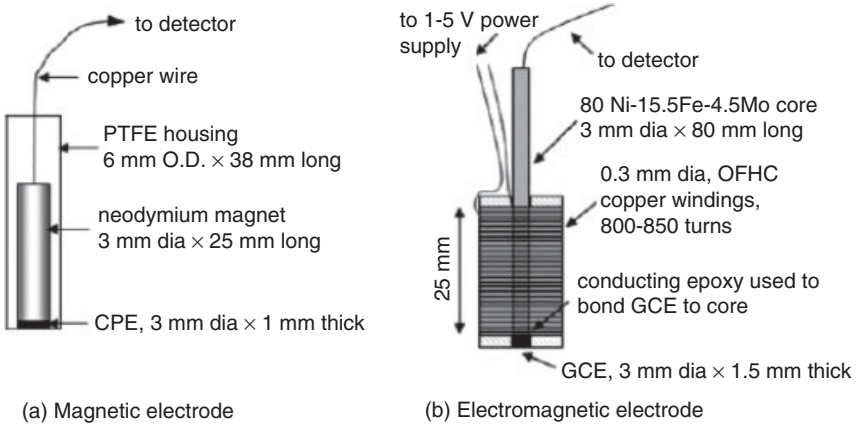

Figure 8.7 Schematic diagrams of (a) magnetic electrode and (b) electromagnetic electrode that preconcentrate metal ions using superparamagnetic nanoparticles. Reprinted with permission from Reference [56]. Copyright 2008 The Royal Society of Chemistry.

proteins present in the sample matrix, leading to a lowered signal response, and (ii) electrode fouling caused by proteins. As can be seen from Figure 8.8, we have successfully measured concentrations of Pb in urine as low as 10 ppb with as little as 20 s of preconcentration (after the optimal 90 s of preconcentration the detection limit dropped to 2.5 ppb Pb).

Furthermore, Figure 8.9 shows that the magnetic nanoparticles can also enable the detection of multiple heavy metals (i.e., Cd, Pb, Cu, and Ag) from various natural river and ocean waters with only ~2.5 min of preconcentration time.

In addition to this work several other groups have reported the use of magnetic nanoparticles in the electrochemical analysis of other environmentally relevant targets (e.g., proteins and nucleic acids) besides heavy metals [21, 22, 65]. The reader is directed to two recent reviews for the application of high surface area magnetic nanomaterials for the detection of biological analytes [20, 66]. Importantly, even though the bulk of the work that has been performed in this area was aimed at clinical applications, the detection of biological species is of paramount importance to environmental sensing due to the biological origin of many common environmental contaminants [67]. A recent example that employs magnetic nanomaterials for the detection of a protein biomarker to pesticide

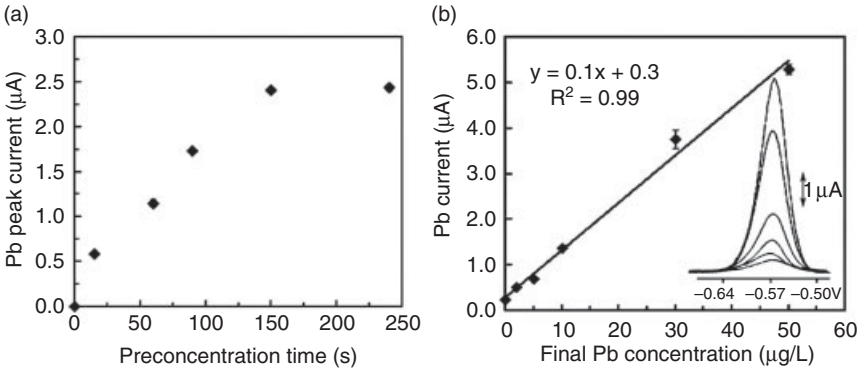

Figure 8.8 (a) Signals of 10 ppb Pb measured at DMSA–Fe_3O_4-magnetic sensors in samples containing 25 vol.% rat urine with varied preconcentration time; (b) linear Pb calibration curve measured at DMSA–Fe_3O_4 magnetic sensors in Pb-spiked samples containing 25 vol.% rat urine. Reprinted with permission from Reference [56]. Copyright 2008 The Royal Society of Chemistry.

Figure 8.9 Sensor measurements of (a) background metal ions in seawater (dashed line) and river water (solid line) and (b) background metal ions (thin line) and metals spiked (thick line) in seawater, after 150 s of preconcentration time. Inset: metal concentrations, measured with ICP-MS, and the distribution coefficients of multiple metal ions (S/L of 0.01 $g\,l^{-1}$ of DMSA–Fe_3O_4, initial metal conc. of 500 ppb each, pH of 7.20 for river water and 7.64 for seawater). Reprinted with permission from Reference [56]. Copyright 2008 The Royal Society of Chemistry.

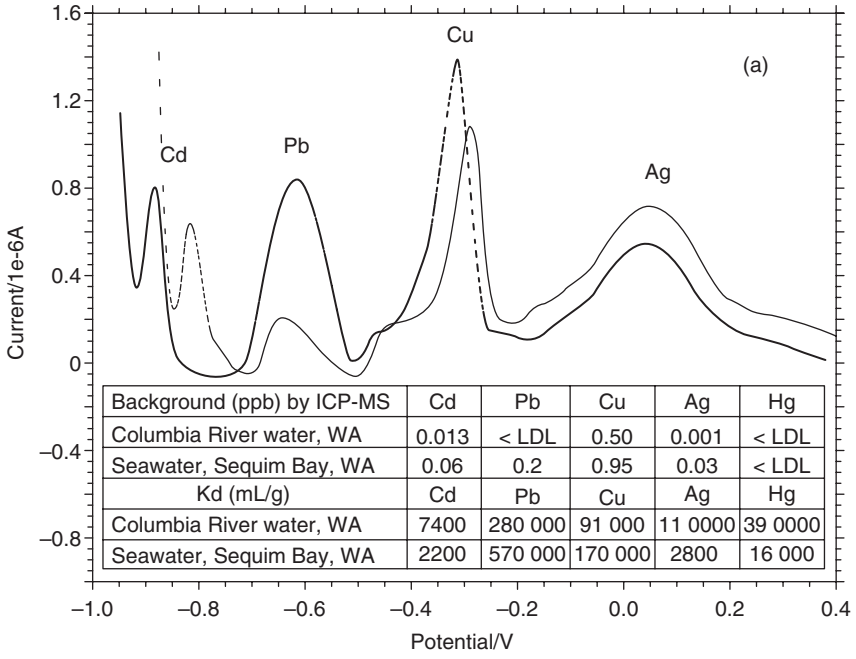

Background (ppb) by ICP-MS	Cd	Pb	Cu	Ag	Hg
Columbia River water, WA	0.013	< LDL	0.50	0.001	< LDL
Seawater, Sequim Bay, WA	0.06	0.2	0.95	0.03	< LDL
Kd (mL/g)	Cd	Pb	Cu	Ag	Hg
Columbia River water, WA	7400	280 000	91 000	11 0000	39 0000
Seawater, Sequim Bay, WA	2200	570 000	170 000	2800	16 000

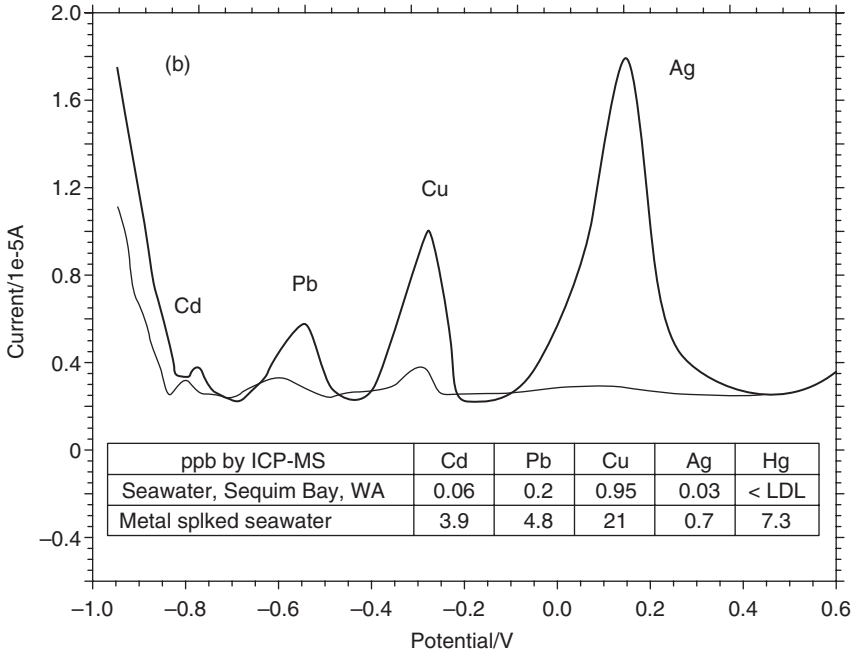

ppb by ICP-MS	Cd	Pb	Cu	Ag	Hg
Seawater, Sequim Bay, WA	0.06	0.2	0.95	0.03	< LDL
Metal splked seawater	3.9	4.8	21	0.7	7.3

exposure utilizes a similar magnetic electrode to that described above and shown in Figure 8.7 [68]. In this work, the magnetic particles have been bound with gold nanoparticles to provide an extremely responsive material for electrochemical analysis [68, 69]. These composite nanomaterials have been used to bind and separate protein biomarker targets from solution followed by detection, obviating the need for the amplification used in typical protein detection [68, 69].

Although the bulk of reported detection schemes focus on the use of magnetic nanoparticles in electrochemical assays, the use of magnetic nanoparticles in trace analyte optical detection scenarios has received a great deal of attention. Recent reviews by Corr *et al.* and Katz *et al.* go into great depth on the formation of nanomaterial composites for biological detection and biomedical applications [18, 21]. Even when one considers all of the potential benefits associated with using a fluorescent nanomaterial that also is magnetic, many complications can arise. Primarily, the use of materials such as magnetic nanoparticles in an optical detection platform can scatter, absorb, or even quench the optical signal from the fluorescent reporter, which leads to a decrease in signal output. Despite this limitation, magnetic/fluorescent materials have great promise in environmental sensing because they will enable separation/preconcentration of target analytes from a complex sample prior to analysis, preventing unwanted optical noise from background interferents. Concurrently, these materials will optically label the target analyte upon binding, allowing for rapid sample analysis using traditional optical methods. We believe that as the materials production methods continue to mature and more magnetic/fluorescent composite nanomaterials become available there will be an explosion in the use of these types of materials in environmental sensing applications.

8.5
Nanoporous Carbon Based Sorbent Materials

Activated carbon is arguably the oldest and most widely utilized sorbent in human history [70]. Activated carbon has been around since antiquity and has grown into a major industry today, enjoying sales of many hundreds of millions of dollars each year. Activated carbon has several features that are attractive for preconcentration of analytes from aqueous systems – it is affordable, widely available, has a high surface area, an open pore structure, is stable towards hydrolysis, has good chemical stability, and excellent thermal stability. Activated carbon is widely used in the removal of various contaminants from water in municipal drinking water purification (e.g., chlorocarbons arising as a by-product of the chlorination process [71]). The utility of activated carbon as a sorbent material is centered around its ability to capture a wide variety of chemical species. Such non-specific adsorption is not necessarily desirable for analytical preconcentration as it entrains many other species that are not of interest and wastes valuable capture capacity doing so. Chemical selectivity can be very valuable for analytical preconcentration.

There have been numerous efforts over the years to chemically modify activated carbon in an effort to enhance its capture efficiency for specific analytes. Many of

these efforts have involved some sort of controlled oxidation, or acid treatment, as a way to increase the degree of oxygenation of the carbon backbone. For example, activated carbon treated with sulfuric acid has been used to adsorb pollutants from wastewater [72]. Activated carbon has also been treated with various oxidants to enhance its adsorption capacity. Treatment of granular activated carbon with potassium bromate has been found to enhance the sorption of Ni ions [73].

8.5.1 Chemically-Modified Activated Carbons

Numerous studies have used chemically modified activated carbons to capture a wide variety of metal ions from aqueous environments. Various activated carbons have been used to capture chromate from wastewater [74]. Similarly, various activated carbons' capture efficiency for Ni^{2+} has been systematically compared [75]. Selective sorption of Pt^{2+} from a mixture of metals in solution was also studied using chemically modified activated carbon [76]. Likewise, toxic metals like Pb^{2+} [77], Cd^{2+} [78] and Cu [79] have all been concentrated from aqueous media using carbon-based sorbents. Activated carbons have even had polymer chains intercalated into their porous architectures in an effort to enhance their ability to bind toxic heavy metals [80].

Chemically modified activated carbons have been used for the preconcentration of specific analytes for water quality analysis. For example, various trace-level toxic elements have been concentrated from water samples for analysis by neutron activation [81, 82]. This area has been reviewed recently [83].

Clearly, activated carbon is a broad-scale sorbent, capable of sorbing a wide variety of analytes. When sampling natural waters, this can lead to undesirable fouling and competition issues. Therefore, it would be desirable to attach specific ligands (as opposed to generic "activation") inside the carbon scaffold so that additional chemical selectivity might be imparted.

Simple ligands have been attached on the carbon backbone to enhance metal binding affinity. For example, activated carbon has been sulfonated to produce a sulfonic acid moieties (Scheme 8.1) that are known to be effective for ion exchange [84]. Activated carbon has also been nitrated, and the nitro groups subsequently reduced to amines (Scheme 8.2), which were then used to capture various transition metals and lanthanide ions from aqueous media [85].

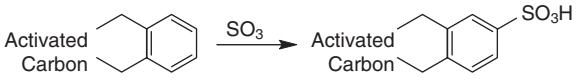

Scheme 8.1

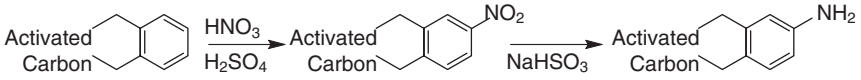

Scheme 8.2

More recently, activated carbon has been chloromethylated, analogous to the synthesis of the polymeric system known as Merrifield's resin [86]. Chloromethylation allows for the easy introduction of a wide variety of chemical functionality through simple substitution reactions (Scheme 8.3). In this case, the chloride was displaced by a sulfur-containing nucleophile, and the resulting thiolated activated carbon was shown to be an effective, and selective, heavy metal sorbent [87]. Table 8.4 compares the performance of thiolated nanoporous carbon with conventional activated carbon. The thiol functionality improves the affinity of the material for softer heavy metals. Notably, a portion of the functionality appears to be located inside micropores (an inherent limitation of activated carbon) and therefore has limited chemical accessibility.

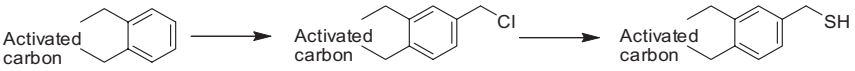

Scheme 8.3

More sophisticated chelating ligands, such as *N,N′*-bis(salicylidene)-1,2-phenylenediamine, have also been immobilized on activated carbon. This sorbent material has been used to capture ultra-trace levels of copper from aquatic media prior to analysis [88]. Moving to a more sophisticated ligand design allows for greater discrimination in the binding chemistry.

Chemically modifying activated carbon has the advantages of being simple and direct. This substrate also has a high surface area and is readily available in bulk. However, this approach is limited due to the microporosity inherent to activated carbon, as well as the latent functionality of the activated carbon backbone (e.g.,

Table 8.4 K_d (ml g^{-1} sorbent) values based metal sorption experiments using thiolated activated carbon (AC-CH_2SH). All experiments were performed in triplicate and averaged. Data reprinted with permissions from Reference [87]. Copyright 2010 Elsevier.

Sorbent	Final pH	Average K_d							
		Co^{2+}	Cu^{2+}	As^{3+}	Ag^{+}	Cd^{2+}	Hg^{2+}	Tl^{+}	Pb^{2+}
AC-CH_2SH	0.17	280	260	180	1700	0	1.6×10^6	96	91
	2.02	160	260	78	1400	83	1.1×10^6	19	120
	4.31	120	2100	0	5800	270	1.8×10^6	110	1500
	6.37	1100	5.5×10^4	160	6.2×10^4	1400	2.2×10^6	560	8.6×10^4
	7.33	1900	1.0×10^5	0	3.4×10^5	5000	6.1×10^6	1500	1.2×10^5
	8.49	2100	8.8×10^4	0	4.1×10^5	4300	2.0×10^7	1700	1.1×10^5
Activated carbon	2.12	0	55	0	220	0	2600	73	170
	4.22	110	5400	0	820	170	4800	250	6600
	7.61	1300	5.3×10^4	23	3400	2900	9700	1800	6.7×10^4

carboxylic acids, phenols, ketones, etc.). Both factors lead to non-selective metal ion (and organic) sorption, and therefore to a significant amount of undesirable competing adsorption. Clearly, it would be advantageous to work with a carbon scaffold having large pores that were constructed around specifically tailored functionality.

8.5.2 Templated Mesoporous Carbons

In recent years a great deal of effort has gone into the study of templated mesoporous carbons [89–100]. This approach generally uses a templated mesoporous silica as scaffold upon which some suitable organic precursor is arrayed, and subsequently polymerized and carbonized (typically at 800–1000 °C). After the carbonization stage, the silica template is generally removed by digestion with either HF or NaOH, leaving a free-standing nanoporous carbon scaffold that is structurally related to the original silica template.

Because of the high temperatures involved in the carbonization stage, this synthetic strategy tends to have very little flexibility in terms of functional "handles" that can be used to bind metal ions, or other analytes. A clever solution to this problem has been reported by Mokaya and coworkers in their syntheses of N-doped mesoporous carbons [97–99]. In this work a stream of acetonitrile (CH_3CN) vapor was entrained in an inert atmosphere and passed through a tube furnace (generally at 900–1100 °C) containing a sample of the silica template. The acetonitrile was carbonized on the silica surface, and the resulting mesoporous carbon was found to contain ~8% N, with a surface area of ~1000 $m^2 g^{-1}$, and a pore volume of 0.83 $cm^3 g^{-1}$. XPS analysis of this material suggests that the N functionality is a mixture of "pyridine-like N" and quaternary ammonium salts. Use of these materials as a sorbent to capture metal ions and other analytes has not yet been demonstrated but pyridine ligands are well known to bind metal ions and quaternary ammonium salts can be used for anion exchange.

High surface area N-containing mesoporous carbons have been made using other strategies as well. It is possible to start with the N-containing arene intact and polymerize the heteroaromatic precursor (Scheme 8.4). For example, 1,10-phenanthroline is a diamine that is well known to chelate various transition metal cations [101]. Utilization of this material in the synthesis of templated mesoporous

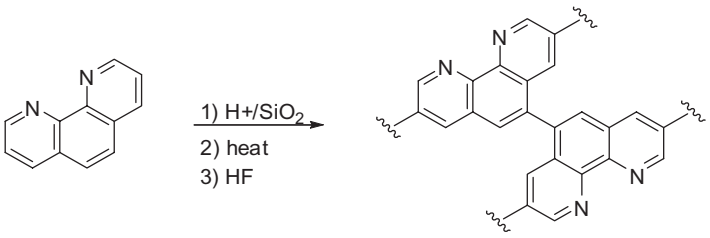

Scheme 8.4

carbon resulted in a product that had a surface area of approximately 870 $m^2 g^{-1}$ and 30–35 Å pores [102]. Owing to the reluctance of the 1,10-phenanthroline nucleus to undergo electrophilic aromatic substitution, this strategy was found to require temperatures of 700–800 °C for carbonization. As a result, N loss (which takes place above about 600 °C [103]) was able to compete and these materials were found to contain ~5% N. This material was found to have excellent chemical and thermal stability and was shown to be an effective sorbent for transition metal cations (e.g., Ni^{2+}).

High surface area pyridine-based mesoporous carbons have also been made using the cyclotrimerization of diethynylpyridines (Scheme 8.5) by taking advantage of the high reactivity of the acetylene group [104]. The structure of products obtained from this approach depended on the regiochemistry of the acetylene groups on the pyridine precursor. The best results were obtained with the 2,5-diethynylpyridine precursor, which gave a product with a surface area of 1930 $m^2 g^{-1}$, a pore volume of 2.14 $cm^3 g^{-1}$, and ~4% N. These high surface area pyridine-based materials have not been evaluated as preconcentration sorbents, but should be useful for capturing transition metal cations, organic acids, and

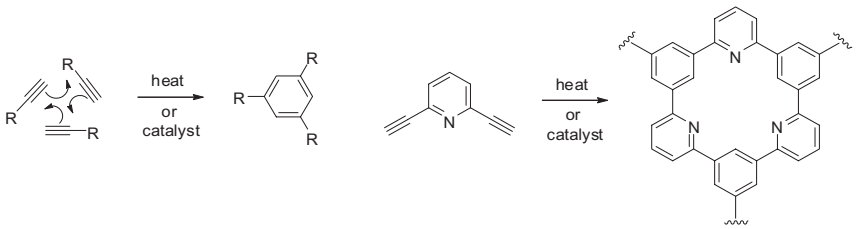

Scheme 8.5

trigonal (or tetrahedral) anions.

The primary limitation of this synthetic strategy is the high temperature required for the polymerization/carbonization process. Above 600 °C, pyridine rings undergo ring–ring fusion reactions and N is lost [103]. Therefore, it would be desirable to use more reactive polymerization chemistry in an effort to lower these temperatures as far as possible so as to preserve as much of the N functionality as possible. $SiCl_4$-catalyzed cyclotrimerization of commercially available 2,6-diacetylpyridine inside an SBA-15 template (Scheme 8.6) has been shown to result in a mesoporous carbon at temperatures as low as 600 °C [105]. The product was found to have a surface area of 1275 $m^2 g^{-1}$, 35 Å pores, and contain 6.8% N. Again, this pyridine-based nanoporous sorbent should be useful for capturing transition metal cations, organic acids, and (in protonated form) trigonal or tetrahedral anions.

Other heteroaromatic precursors can also be used in this chemistry. For example, acid-catalyzed polymerization of 2-thiophenemethanol inside an SBA-15 template (Scheme 8.7), and subsequent carbonization of the intermediate product at 700–800 °C, was found to create a S-functionalized mesoporous carbon (S-FMC) [106].

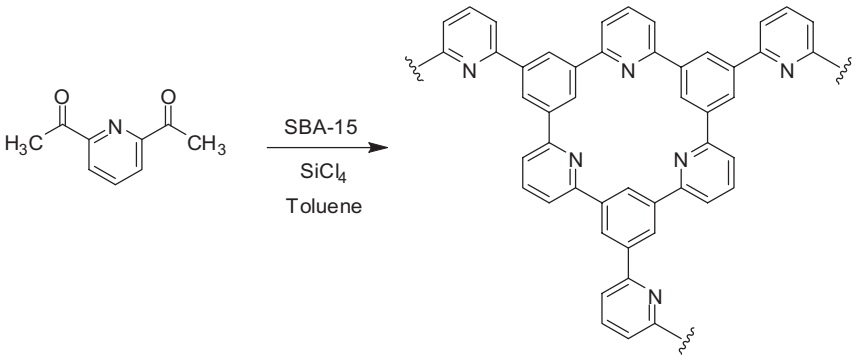

Scheme 8.6

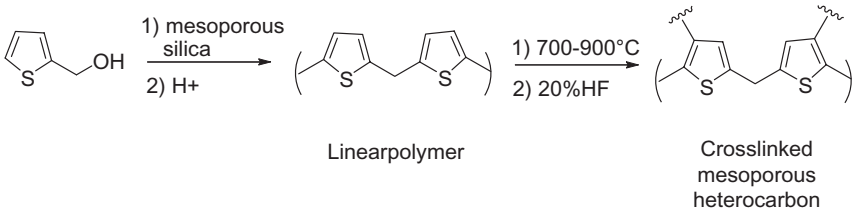

Scheme 8.7

The S content, surface area, and pore volume depended on the carbonization temperature, but between 700 and 800 °C, the S content was 4.9–7.2%, the surface area was 1620–1930 $m^2 g^{-1}$, and the pore volume was 1.68–2.14 $cm^3 g^{-1}$. Like all mesoporous carbons, these S-FMCs showed excellent thermal and chemical stability; boiling them in buffers from pH 1 to 13 for 24 h induced no discernible change. Indeed, these S-FMCs were found to be effective heavy metal sorbents. The K_ds for Hg^{2+} were >250 000 over the same broad range of pH (1–13). Very few heavy metal sorbents are capable of effective metal capture over such a wide range of pH.

One of the advantages of carbon-based sorbents is their chemical stability and resistance to chemical degradation. Unfortunately, this chemical stability also means that they are resistant to several commonly used forms of chemical functionalization. Such chemical functionalization is needed to augment their poor selectivity. Chemical selectivity is desirable for analytical preconcentration applications (and also in remediation applications) so as not to consume the sorbent's capacity to bind non-target species. Installation of specific ligand chemistries (e.g., thiols, thiophenes, chelating diamines, etc.) helps to overcome this shortcoming. These solutions preserve the chemical stability of the carbon backbone while adding chemically selective ligands with improved affinity for metal species, and extend the usefulness of carbon-based sorbents beyond that of a general sorbent.

8.6
Other Nanostructured Sorbent Materials

8.6.1
Zeolites

Zeolites are aluminosilicate materials that exhibit well-defined, highly porous structures. They occur naturally and may be prepared by several methods. The general zeolite structure is a three-dimensional network of repeating isomorphous SiO_4 and AlO_4^- tetrahedra linked by oxygen atoms (Figure 8.10). This yields an anionic lattice with acidic (bridging OH groups on Al–O–Si linkages) and basic (Al tetrahedra) sites. Charge balance is maintained by extra-lattice Na^+, K^+, Ca^{2+}, or Mg^{2+} atoms. To date, there are over 40 different naturally occurring zeolites that differ in structure and in Al : Si ratio [107]. Small amounts of Fe are also found in natural zeolites [108].

Zeolites are widely used in both separation and catalysis applications [109]. Like activated carbon materials, zeolites are commonly employed as general sorbents [110]. Their high surface area allows removal of organic species from solution although their effectiveness as sorbents for organic species is limited compared to that of activated carbon materials [110]. Their anionic framework makes zeolites natural cation exchangers while their well-defined pores lend some degree of preference to the ions absorbed. The most widely-used and studied natural zeolite, clinoptilolite, exhibits a general selectivity: $Pb^{2+} > Cd^{2+} > Cs^+ > Co^{2+} > Cr^{3+} > Zn^{2+} > Ni^{2+} > Hg^{2+}$ [111]. Clinoptilolite is also effective in sorption of Sr^{2+} and

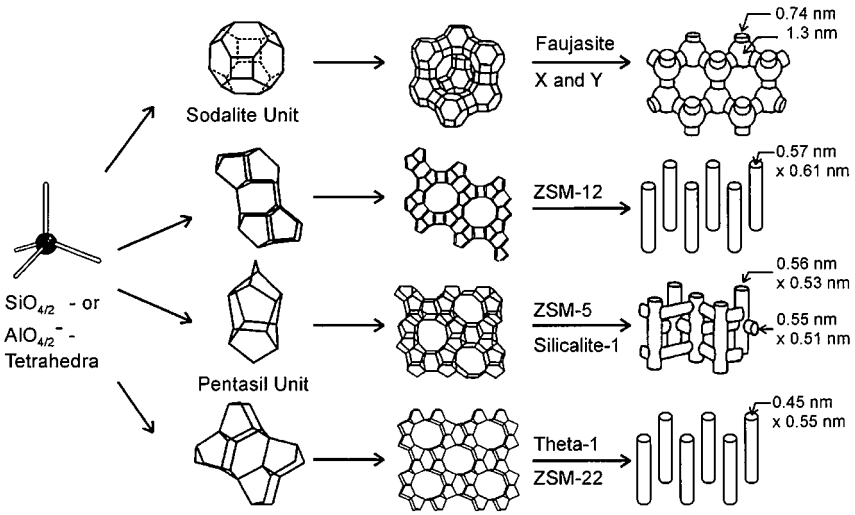

Figure 8.10 Structures of several zeolites as well as their pore shapes and dimensions. Reprinted with permission from Reference [115]. Copyright 2000 Elsevier.

Sb^{2+} cations [112, 113]. Other natural zeolite materials may differ in selectivity. For instance, scolecite follows the series $Cr^{3+} > Mn^{2+} > Cd^{2+} > Ni^{2+}$ [114]. This selectivity is desirable for adsorption of these analytes at trace levels in matrices that contain competing species.

Adsorption of metals by zeolites is governed by pH, temperature, and is made further complex by the different surface sites found within the lattices. The pH affects not only the state of lattice hydroxyl groups and metal speciation but, at very low pH, protonation of surface sites reduces the lattice affinity for positively charged species [116].

Analysis of adsorption isotherms indicates that adsorption of many metal cations occurs via by both ion exchange and chemisoprtion processes. For Pb^{2+} and Zn^{2+} ion exchange occurs quickly and is followed by slower chemisorption [113, 117, 118]. In most cases, sorption favors cations with higher charges and smaller radii [119].

Adsorption occurs most effectively for metals that exist as cations. Because they have little affinity for the anionic lattice, metals that form oxoanions or other anionic species are not as effectively adsorbed. Organic contaminants such as phenol that form complexes with metal ions interfere to various degrees with metal sorption [120]. It is likely that these metal–ligand complexes hinder penetration into pores or form neutral or anionic complexes that have no affinity for the anionic lattice. In some cases, the sorbent may be regenerated with high concentrations of competing cations, such as in solutions of $NaNO_3$. Acid may also be used to strip adsorbed metals, although this has been shown to damage some zeolites [116].

Natural zeolites may be modified to enhance their ability to absorb anionic species. When treated with Fe^{2+} and Fe nanoparticles, these functionalized materials show impressive affinity for arsenate and arsenite anions compared to the native zeolite [121, 122]. Fe^{2+} is also used to treat activated carbon to achieve the same effect [121]. An Al-functionalized zeolite has also been shown to remove arsenate [123]. The small size of natural zeolite pores (typically between 0.4 and 1.2 nm) lends them their selectivity and high surface area but limits their use for adsorption of larger molecules, restricts mass transport through the material, and can result in high back pressure in flow systems [124].

Synthetic zeolites have been designed in an effort to prepare zeolites and zeolite-like materials without these limitations. Two strategies have been explored: (i) making zeolites with larger pores and (ii) inserting larger pores into zeolite materials. These modified zeolites have been reviewed recently [125, 126]. Synthetic mesoporous zeolites may possess different metal selectivity profiles than their natural counterparts. However, little work has been done involving synthetic zeolites as sorbents.

Like activated carbon materials, zeolites are low-cost, high surface area, semi-selective sorbents. Their selectivity can be tailored by modifying lattice constituents, by functionalizing the lattice, or by changing the porous network topology. Like the functionalized nanoporous materials discussed in this section, the high cost of functionalization renders the more sophisticated materials

less practical as sorbents for remediation but makes them ideal for detection applications [127].

8.6.2 Ion-Imprinted Polymers

Molecular imprinting is a technique for preparing polymeric matrices that are capable of highly selective solid-phase extraction. Imprinted polymers are prepared by polymerizing functional and often crosslinkable monomers in the presence of an imprint molecule. This preparation of imprinted polymers is typically divided into three steps (Figure 8.11). During an imprint step, functional monomers form a complex with the imprint molecule which either closely resembles or is identical to a target analyte. The monomers are then crosslinked during a polymerization step. This fixes their position and orientation in the network. The imprint molecule is then removed during a leaching step. The polymer network is left with functional monomers pre-organized in a geometry optimum for binding the template molecule.

The first ion-imprinted polymer was developed by Nishide *et al*. in 1976 [129, 130]. These early poly(4-vinlypyridine) resins could be imprinted to preferentially adsorb Cu^{2+}, Ni^{2+}, Hg^{2+}, Zn^{2+}, and Cd^{2+}. Since then, efforts have been made to selectively bind different metals, improve the efficiency of absorption, and develop robust, regenerable imprinted polymers. Many of these efforts have involved incorporating metal chelating systems into polymer matrices. For example, carboxylic acid derivatized monomers have been shown to produce a resin specific to UO_2^{2+} [131]. 5,7-Dichloroquinoline derivatives have been used as the chelating monomers for Dy- and Sm^{3+}-specific polymers [132, 133]. A polymerizable 3-oxapentanediamide derivative was employed in a polymer that could be used to

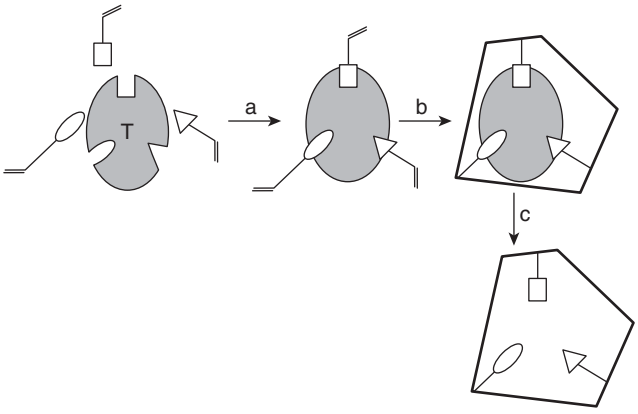

Figure 8.11 Representation of imprinting process: (a) complexation; (b) polymerization; (c) leaching. T = imprint molecule. Reprinted with permission from Reference [128]. Copyright 2004 Elsevier.

separate Ca^{2+} from Mg^{2+} ions and vice versa [134]. Lemaire, *et al*. have used methacrylate monomers to selectively bind Gd and, in a similar polymer matrix, diethylene triamine pentaacetic acid (DPTA) derivative chelating monomers for La^{3+} [135]. Prasada Rao *et al*. have reviewed this topic recently [128, 136].

Since adsorption of metal ions by ion-imprinted polymers is governed almost entirely by chemisorption, using more sophisticated ligands yields higher specificity and more efficient adsorption of target analytes. The synthetic challenges have been to incorporate these sophisticated chelate functionalities into polymerizable molecules. It is sometimes possible to circumvent this challenge by using both polymerizable and non-polymerizable ligands to form the template–ligand complex. The non-polymerizable ligands becomes trapped in the polymer matrix even after the template species is removed [136].

Advantages of imprinted polymers are simple preparation, durability, and predetermined and predictable selectivity. They may be used as bulk polymer, but are more effective when incorporated into nanostructured materials. Ion-imprinted polymers may be cast as thin films, incorporated into membranes, or applied as coatings to solid supports [127, 129–132]. Applying the polymer to a high surface area material eliminates the mass transport limitation involved in using the material in bulk. Drawbacks to ion-imprinted polymers involve poor solubility of the template (metal ion) in the imprinting mixture.

This section has outlined just two particular classes of material that are being explored for trace metal adsorption from aqueous matrices. There is tremendous room for development of zeolites, ion-imprinted polymer-based materials, and other nanoporous materials like aluminophosphate materials and metal organic frameworks as sorbents for trace-level metal contaminants. Practical utilization of these nanomaterials in trace-level assay will depend upon the capability to tailor the materials into form factors that allow integration with devices and functionalize the surfaces to have high selectivity and affinity.

8.7 Concluding Thoughts

We have reviewed selected nanostructured materials, many with thiol functionalization, for the capture of softer heavy metals from aqueous systems for environmental and sensing and separation applications. It has been clearly shown that correctly constructed nanomaterials can be superior sorbents over conventional materials. These nanomaterials can be used for analytical and remediation applications. It should be reiterated that we chose to emphasize work employing thiol surface chemistry, since it provides a highly effective means for the capture of many toxic heavy metals from aqueous systems and it offers a useful baseline for comparing the performance of the various nanomaterials. Many other elegant surface chemistries exist and enable the use of these nanomaterials for applications to other analyte sets. Beyond simple performance, one remaining factor that merits discussion is the economics of using nanomaterials for collection and detection.

Nanostructured materials can be expensive. While industrial scale-up can bring the cost down, it does not address two fundamental problems. First, scaling the production volumes up from laboratory beakers to industrial tonnage is a non-trivial effort, particularly for advanced materials with complex structures. Second, the materials and methods needed to assemble sorbents with the useful nanostructure and surface chemistry will almost inevitably make them more expensive than bulk or traditional materials. For large-scale applications of nanomaterials, such as environmental remediation efforts, the performance of the materials must be sufficient to merit the additional cost. Viability will have to be assessed on a case by case basis, but will likely be more successful on high value applications such as those associated with nuclear materials or localized applications such as batch treatment. The much larger K_d and capacity values for functionalized nanoporous silica and nanoparticulate iron oxide shown in Tables 8.1, 8.2 and 8.4 suggest that despite higher costs than tradition bulk sorbents they may provide better value for select applications. Furthermore, the possibility of non-covalent modification of SAMMS and related nanomaterials (as in the chemisorbed phenyl-SAMMS materials described in Section 8.3.1) provides a route to mitigate the cost of the nanomaterial by providing a greater product lifetime and sorption capacity.

In contrast to large-scale separations, analytical applications require much smaller volumes of sorbent materials. In most cases analytical applications will require only milligrams (or conceivably even micrograms) of sorbent material and the material might be used for many repeated measurements. Information coming from analytical assays forms the basis for many high value decisions such as those made as a result of medical diagnostics, legal forensics, determination of clean water and food, or operation of an industrial process. Consequently, with high value results and small quantities of material needed, the cost of the sorbent material for analytical applications is generally irrelevant. For analytical applications, obtaining a stable supply of materials with dependable performance and effectively integrating them into the analytical method/device is more important than the nanomaterial cost. For some nanomaterials, such as quantum dot emitters and PANAM dendrimers, reliable industrial production and their wide spread analytical utilization has already been demonstrated. As commercial sources of nanomaterials become increasing available it is inevitable they will be integrated in the products as appropriate, with high value niche applications such as improved analytical devices/methods leading the way.

In conclusion, we have briefly discussed the material science and application of functionalized nanoporous silica, functionalized superparamagnetic particles, nanostructured carbon-based materials, and other structured materials such as zeolites. These materials only scratch the surface of possible nanomaterials that can be employed in sensing and remediation applications. Additional materials that are presently under development, as well as others not yet imagined, will provide new and relevant capabilities, enabling a range of analytical applications for trace-level measurements.

Acknowledgments

Funding for this work was provided in part by the Safer Nanomaterials Nanomanufacturing Initiative (SNNI) of Oregon Nanoscience and Microtechnologies Institute (ONAMI) and Pacific Northwest National Laboratory (PNNL). A portion of this research was performed using Environmental Molecular Sciences Laboratory (EMSL), a national scientific user facility sponsored by the Department of Energy's Office of Biological and Environmental Research located at PNNL. PNNL is operated for the U.S. Department of Energy by Battelle under contract DE-AC06-67RLO 1830. This work was also supported by grants from NIAID (R01-AI080502), NIOSH (1R21 OH008900), and NIEHS (R21-ES015620) and PNNL's LDRD program. Its contents are solely the responsibility of the authors and do not necessarily represent the official views of NIH.

D. W. J, S. A. F., and T. G. C. gratefully acknowledge support from the University of Oregon and an NSF-CAREER award (CHE-0545206). D. W. J is a Cottrell Scholar of Research Corporation. T. G. C. and S. A. F. acknowledge the National Science Foundation (NSF) for Integrative Graduate Education and Research Traineeships (DGE-0549503).

References

1 Poole, C.F. (2003) *Trends Anal. Chem.*, **22**, 362–373.
2 Fryxell, G.E., Lin, Y., Fiskum, S., Birnbaum, J.C., Wu, H., Kemner, K., and Kelly, S. (2005) *Environ. Sci. Technol.*, **39**, 1324–1331.
3 Fryxell, G.E., Liu, J., Mattigod, S.V., Wang, L.Q., Gong, M., Hauser, T.A., Lin, Y., Ferris, K.F., and Feng, X. (2000) in, *Environmental Issues and Waste Management Technologies in the Ceramic and Nuclear Industries V*, (eds G.T. Chandler and X. Feng), Ceramics Transactions, Vol. **107**, The American Ceramic Society, Westerville, OH, pp. 29–37.
4 Fryxell, G.E., Lin, Y., Wu, H., and Kemner, K.M. (2002), in *Studies in Surface Science and Catalysis*, Vol. **141** (eds A. Sayari and M. Jaroniec), Elsevier Science, pp. 583–590.
5 Fryxell, G.E., Addleman, R.S., Mattigod, S.V., Lin, Y., Zemanian, T.S., Wu, H., Birnbaum, J.C., Liu, J., and Feng, X. (2004) in *Dekker Encyclopedia of Nanoscience and Nanotechnology* (ed. J.A. Schwarz), Marcel Dekker, pp. 1135–1145.
6 Mellor, D.P. (1979) *Chemistry of Chelation and Chelating Agents*, Pergamon Press, New York.
7 Richens, D.T. (1997) *The Chemistry of Aqua Ions*, John Wiley & Sons, Ltd, Chichester.
8 Pearson, R.G. (1963) *J. Am. Chem. Soc.*, **85**, 3533–3539.
9 Herrin, R.T., Andren, A.W., Shafer, M.M., and Armstrong, D.E. (2001) *Environ. Sci. Technol.*, **35**, 1959–1966.
10 Powell, K.J., Brown, P.L., Byrne, R.H., Gajda, T., Hefter, G., Sjöberg, S., and Wanner, H. (2004) *Aust. J. Chem.*, **57**, 993–1000.
11 Byrne, R.H. (2002) *Geochem. Trans.*, **3**, 11–16.
12 Yantasee, W., Charnhattakorn, B., Fryxell, G.E., Lin, Y., Timchalk, C., and Addleman, R.S. (2008) *Anal. Chim. Acta*, **620**, 55–63.
13 Yantasee, W., Warner, C.L., Sangvanich, T., Addleman, R.S., Carter, T.G., Wiacek, R.J., Fryxell, G.E., Timchalk, C., and Warner, M.G. (2007) *Environ. Sci. Technol.*, **41**, 5114–5119.

14 Lloyd-Jones, P.J., Rangel-Mendez, J.R., and Streat, M. (2004) *Process Saf. Environ. Prot.*, **82**, 301–311.

15 Carter, T.G., Yantasee, W., Sangvanich, T., Fryxell, G.E., Johnson, D.W., and Addleman, R.S. (2008) *Chem. Commun.*, 5583–5585.

16 United States Pharmacopeia (1990) *USP United States Pharmacopeial Convention Inc.*, 22nd edn, United States Pharmacopeia, Rockville, MD.

17 Shargel, L., and Yu, A.B.C. (2002) *Encyclopedia of Pharmaceutical Technology*, Vol. **1**, 2nd edn (eds J. Swarbrick and J.C. Boylan), Informa Health Care, p. 164.

18 Corr, S.A., Rakovich, Y.P., and Gun'ko, Y.K. (2008) *Nanoscale Res. Lett.*, **3**, 87–104.

19 Hsing, I.M., Xu, Y., and Zhao, W. (2007) *Electroanalysis*, **19**, 755–768.

20 Huber, D.L. (2005) *Small*, **1**, 482–501.

21 Katz, E. and Willner, I. (2004) *Angew. Chem. Int. Ed.*, **43**, 6042–6108.

22 Katz, E., Willner, I., and Wang, J. (2004) *Electroanalysis*, **16**, 19–44.

23 Latham, A.H. and Williams, M.E. (2008) *Acc. Chem. Res.*, **41**, 411–420.

24 Laurent, S., Forge, D., Port, M., Roch, A., Robic, C., Vander Elst, L., and Muller, R.N. (2008) *Chem. Rev.*, **108**, 2064–2110.

25 Lu, A.H., Salabas, E.L., and Schueth, F. (2007) *Angew. Chem. Int. Ed.*, **46**, 1222–1244.

26 Magnani, M., Galluzzi, L., and Bruce, I.J. (2006) *J. Nanosci. Nanotechnol.*, **6**, 2302–2311.

27 Pankhurst, Q.A. (2006) *BT Technol. J.*, **24**, 33–38.

28 Pankhurst, Q.A., Connolly, J., Jones, S.K., and Dobson, J. (2003) *J. Phys. D Appl. Phys.*, **36**, R167–R181.

29 Rodriguez-Mozaz, S., de Alda, M.J.L., and Barcelo, D. (2006) *Anal. Bioanal. Chem.*, **386**, 1025–1041.

30 Salgueirino-Maceira, V. and Correa-Duarte, M.A. (2007) *Adv. Mater.*, **19**, 4131–4144.

31 Seydack, M. (2005) *Biosens. Bioelectron.*, **20**, 2454–2469.

32 Tartaj, P., Morales, M.D., Veintemillas-Verdaguer, S., Gonzalez-Carreno, T., and Serna, C.J. (2003) *J. Phys. D Appl. Phys.*, **36**, R182–R197.

33 Yantasee, W., Lin, Y., Hongsirikarn, K., Fryxell, G.E., Addleman, R.S., and Timchalk, C. (2007) *Environ. Health Perspect.*, **115**, 1683–1690.

34 Cushing, B.L., Kolesnichenko, V.L., and O'Connor, C.J. (2004) *Chem. Rev.*, **104**, 3893–3946.

35 Jun, Y., Choi, J., and Cheon, J. (2006) *Angew. Chem. Int. Ed.*, **45**, 3414–3439.

36 Neouze, M.A. and Schubert, U. (2008) *Monatsh. Chem.*, **139**, 183–195.

37 Park, J., Joo, J., Kwon, S., Jang, Y., and Hyeon, T. (2007) *Angew. Chem. Int. Ed.*, **46**, 4630–4660.

38 Deng, Y.-H., Wang, C.-C., Hu, J.-H., Yang, W.-L., and Fu, S.-K. (2005) *Colloids Surf. A*, **262**, 87–93.

39 Ennas, G., Musinu, A., Piccaluga, G., Zedda, D., Gatteschi, D., Sangregorio, C., Stanger, J.L., Concas, G., and Spano, G. (1998) *Chem. Mater.*, **10**, 495–502.

40 Lu, C.W., Hung, Y., Hsiao, J.K., Yao, M., Chung, T.H., Lin, Y.S., Wu, S.H., Hsu, S.C., Liu, H.M., Mou, C.Y., Yang, C.S., Huang, D.M., and Chen, Y.C. (2007) *Nano Lett.*, **7**, 149–154.

41 Santra, S., Tapec, R., Theodoropoulou, N., Dobson, J., Hebard, A., and Tan, W. (2001) *Langmuir*, **17**, 2900–2906.

42 Stober, W., Fink, A. and Bohn, E. (1968) *J. Colloid Interface Sci.*, **26**, 62–69.

43 Carpenter, E.E. (2001) *J. Magn. Magn. Mater.*, **225**, 17–20.

44 Mikhaylova, M., Kim, D.K., Bobrysheva, N., Osmolowsky, M., Semenov, V., Tsakalakos, T., and Muhammed, M. (2004) *Langmuir*, **20**, 2472–2477.

45 Lo, C.K., Xiao, D., and Choi, M.M.F. (2007) *J. Mater. Chem.*, **17**, 2418–2427.

46 Lu, Q.H., Yao, K.L., Xi, D., Liu, Z.L., Luo, X.P., and Ning, Q. (2006) *J. Magn. Magn. Mater.*, **301**, 44–49.

47 Mandal, M., Kundu, S., Ghosh, S.K., Panigrahi, S., Sau, T.K., Yusuf, S.M., and Pal, T. (2005) *J. Colloid Interface Sci.*, **286**, 187–194.

48 Park, H.Y., Schadt, M.J., Wang, L.Y., Lim, I.I.S., Njoki, P.N., Kim, S.H.,

Jang, M.Y., Luo, J., and Zhong, C.J. (2007) *Langmuir*, **23**, 9050–9056.
49 Lim, J., Eggeman, A., Lanni, F., Tilton, R.D., and Majetich, S.A. (2008) *Adv. Mater.*, **20**, 1721–1726.
50 Xu, Z., Hou, Y., and Sun, S. (2007) *J. Am. Chem. Soc.*, **129**, 8698–8699.
51 Wang, L., Luo, J., Maye, M.M., Fan, Q., Rendeng, Q., Engelhard, M.H., Wang, C., Lin, Y., and Zhong, C.-J. (2005) *J. Mater. Chem.*, **15**, 1821–1832.
52 Gong, P., Li, H., He, X., Wang, K., Hu, J., Tan, W., Zhang, S., and Yang, X. (2007) *Nanotechnology*, **18**, 285604.
53 Kimishima, Y., Yamada, W., Uehara, M., Asaka, T., Kimoto, K., and Matsui, Y. (2007) *Mater. Sci. Eng. B*, **138**, 69–73.
54 Tang, D.P., Yuan, R., and Chai, Y.Q. (2006) *J. Phys. Chem. B*, **110**, 11640–11646.
55 Liu, C., Zhou, Z., Yu, X., Lv, B., Mao, J., and Xiao, D. (2008) *Inorg. Mater.*, **44**, 291–295.
56 Yantasee, W., Hongsirikarn, K., Warner, C.L., Choi, D., Sangvanich, T., Toloczko, M.B., Warner, M.G., Fryxell, G.E., Addleman, R.S., and Timchalk, C. (2008) *Analyst*, **133**, 348–355.
57 Santandreu, M., Sole, S., Fabregas, E., and Alegret, S. (1998) *Biosens. Bioelectron.*, **13**, 7–17.
58 Riskin, M., Basnar, B., Huang, Y., and Willner, I. (2007) *Adv. Mater.*, **19**, 2691–2693.
59 Liu, H.B., Guo, J., Jin, L., Yang, W.L., and Wang, C.C. (2008) *J. Phys. Chem. B*, **112**, 3315–3321.
60 Cai, J., Guo, J., Ji, M.L., Yang, W.L., Wang, C.C., and Fu, S.K. (2007) *Colloid Polym. Sci.*, **285**, 1607–1615.
61 Shin, S. and Jang, J. (2007) *Chem. Commun.*, 4230–4232.
62 Ngomsik, A., Bee, A., Draye, M., Cote, G., and Cabuil, V. (2005) *C. R. Chim.*, **8**, 963–970.
63 Yavuz, C.T., Mayo, J.T., Yu, W.W., Prakash, A., Falkner, J.C., Yean, S., Cong, L.L., Shipley, H.J., Kan, A., Tomson, M., Natelson, D., and Colvin, V.L. (2006) *Science*, **314**, 964–967.
64 Yean, S., Cong, L., Yavuz, C.T., Mayo, J.T., Yu, W.W., Kan, A.T., Colvin, V.L., and Tomson, M.B. (2005) *J. Mater. Res.*, **20**, 3255–3264.
65 Palecek, E. and Fojta, M. (2007) *Talanta*, **74**, 276–290.
66 de la Escosura-Muniz, A., Ambrosi, A., and Merkoci, A. (2008) *Trends Anal. Chem.*, **27**, 568–584.
67 EPA (2010) Drinking water contaminants, http://www.epa.gov/ogwdw/hfacts.html (accessed 20 January 2010).
68 Liu, G.D., Timchalk, C., and Lin, Y.H. (2006) *Electroanalysis*, **18**, 1605–1613.
69 Liu, G. and Lin, Y. (2005) *J. Nanosci. Nanotechnol.*, **5**, 1060–1065.
70 Bansal, R.C. and Goyal, M. (2005) *Activated Carbon Adsorption*, Taylor & Francis, New York.
71 Pelech, R., Milchert, E., and Bartkowiak, M. (2006) *J. Colloid Interface Sci.*, **296**, 458–464.
72 Jiang, Z.X., Liu, Y., Sun, X.P., Tian, F.P., Sun, F.X., Liang, C.H., You, W.S., Han, C.R., and Li, C. (2003) *Langmuir*, **19**, 731–736.
73 Satapathy, D. and Natarajan, G.S. (2006) *Adsorption - J. Int. Adsorption Soc.*, **12**, 147–154.
74 Babel, S. and Kurniawan, T.A. (2004) *Chemosphere*, **54**, 951–967.
75 Kannan, N. and Rengasamy, G. (2005) *Fresenius Environ. Bull.*, **14**, 435–443.
76 Kasaini, H., Everson, R.C., and Bruinsma, O.S.L. (2005), *Sep. Sci. Technol.*, **40** (1–3), 507–523.
77 Abdulkarim, M. and Abu Al-Rub, F. (2004) *Adsorption Sci. Technol.*, **22**, 119–134.
78 Rangel-Mendez, J.R. and Streat, M. (2002) *Water Res.*, **36**, 1244–1252.
79 Biniak, S., Pakula, M., Szymanski, G.S., and Swiatkowski, A. (1999) *Langmuir*, **15**, 6117–6122.
80 Yin, C.Y., Aroua, M.K., and Daud, W. (2007) *Colloids Surf. A*, **307**, 128–136.
81 Yusof, A.M., Rahman, M.M., and Wood, A.K.H. (2004) *J. Radioanal. Nucl. Chem.*, **259**, 479–484.
82 Yusof, A.M., Rahman, M.M., and Wood, A.K.H. (2007) *J. Radioanal. Nucl. Chem.*, **271**, 191–197.
83 Yin, C.Y., Aroua, M.K., and Daud, W. (2007) *Sep. Purif. Technol.*, **52**, 403–415.

84 Yantasee, W., Lin, Y.H., Alford, K.L., Busche, B.J., Fryxell, G.E., and Engelhard, M.H. (2004) *Sep. Sci. Technol.*, **39**, 3263–3279.

85 Yantasee, W., Lin, Y.H., Fryxell, G.E., Alford, K.L., Busche, B.J., and Johnson, C.D. (2004) *Ind. Eng. Chem. Res.*, **43**, 2759–2764.

86 Merrifield, R.B. (1963) *J. Am. Chem. Soc*, **85**, 2149.

87 Samuels, W.D., LaFemina, N.H., Sukwarotwat, V., Yantasee, W., Li, X.S., and Fryxell, G.E. (2010) *Sep. Sci. Technol.*, **45**, 228–235.

88 Gholivand, M.B., Ahmadi, F., and Rafiee, E. (2007) *Sep. Sci. Technol.*, **42**, 897–910.

89 Ryoo, R., Joo, S.H., and Jun, S. (1999) *J. Phys. Chem. B*, **103**, 7743–7746.

90 Joo, S.H., Choi, S.J., Oh, I., Kwak, J., Liu, Z., Terasaki, O., and Ryoo, R. (2001) *Nature*, **412**, 169–172.

91 Gierszal, K.P. and Jaroniec, M. (2006) *J. Am. Chem. Soc*, **128**, 10026–10027.

92 Lee, J., Sohn, K., and Hyeon, T. (2001) *J. Am. Chem. Soc*, **123**, 5146–5147.

93 Kim, C.H., Lee, D.K., and Pinnavaia, T.J. (2004) *Langmuir*, **20**, 5157–5159.

94 Lu, A.H., Kiefer, A., Schmidt, W., and Schuth, F. (2004) *Chem. Mater.*, **16**, 100–103.

95 Liang, C.D. and Dai, S. (2006) *J. Am. Chem. Soc*, **128**, 5316–5317.

96 Wang, X.Q., Liang, C.D., and Dai, S. (2008) *Langmuir*, **24**, 7500–7505.

97 Xia, Y.D. and Mokaya, R. (2005) *Chem. Mater.*, **17**, 1553–1560.

98 Xia, Y.D., Yang, Z.X., and Mokaya, R. (2004) *J. Phys. Chem. B*, **108**, 19293–19298.

99 Yang, Z.X., Xia, Y.D., Sun, X.Z., and Mokaya, R. (2006) *J. Phys. Chem. B*, **110**, 18424–18431.

100 Fulvio, P.F., Jaroniec, M., Liang, C.D., and Dai, S. (2008) *J. Phys. Chem. C*, **112**, 13126–13133.

101 Cotton, F.A. and Wilkinson, G. (1980) *Advanced Inorganic Chemistry*, 4th edn, John Wiley & Sons, Inc., New York.

102 Shin, Y., Fryxell, G.E., Engelhard, M.H., and Exarhos, G.J. (2007) *Inorg. Chem. Commun.*, **10**, 1541–1544.

103 Bahl, O.P., Shen, Z., Lavin, J.G., and Ross, R.A. (1998) *Carbon Fibers*, 3rd edn (eds S. Rebouillat, J.B. Donnet, T.K. Wang, and J.C.M. Peng), Marcel Dekker, New York, pp. 1–83.

104 Shin, Y., Fryxell, G.E., Johnson, C.A., and Haley, M.M. (2008) *Chem. Mater.*, **20**, 981–986.

105 Shin, Y., Wang, C., Engelhard, M.H., and Fryxell, G.E. (2009) *Microporous Mesoporous Mater.*, **123**, 345–348.

106 Shin, Y.S., Fryxell, G., Um, W.Y., Parker, K., Mattigod, S.V., and Skaggs, R. (2007) *Adv. Funct. Mater.*, **17**, 2897–2901.

107 Baerlocher, C., Meier, W.M., and Olson, D.H. (2001) *Atlas of Zeolite Framework Types*, 5th edn, Elsevier, Amsterdam.

108 Erdem, E., Karapinar, N., and Donat, R. (2004) *J. Colloid Interface Sci.*, **280**, 309–314.

109 Hartmann, M. and Kevan, L. (1999) *Chem. Rev.*, **99**, 635–664.

110 San Miguel, G., Lambert, S.D., and Graham, N.J.D. (2006) *J. Chem. Technol. Biotechnol.*, **81**, 1685–1696.

111 Zamzow, M.J., Eichbaum, B.R., Sandgren, K.R., and Shanks, D.E. (1990) *Sep. Sci. Technol.*, **25** (13-15), 1555–1569.

112 Um, W. and Papelis, C. (2004) *Environ. Sci. Technol.*, **38**, 496–502.

113 Um, W. and Papelis, C. (2003) *Am. Mineral.*, **88**, 2028–2039.

114 Dal Bosco, S.M., Jimenez, R.S., and Carvalho, W.A. (2005) *J. Colloid Interface Sci.*, **281**, 424–431.

115 Weitkamp, J. (2000) *Solid State Ionics*, **131**, 175–188.

116 Wingenfelder, U., Hansen, C., Furrer, G., and Schulin, R. (2005) *Environ. Sci. Technol.*, **39**, 4606–4613.

117 Shahwan, T., Zünbül, B., Tunusoglu, Ö., and Eroglu, A.E. (2005) *J. Colloid Interface Sci.*, **286**, 471–478.

118 Ören, A.H. and Kaya, A. (2006) *J. Hazard. Mater.*, **131**, 59–65.

119 Logar, N.Z. and Kaucic, V. (2006) *Acta Chim. Slov.*, **53**, 117–135.

120 Vaca Mier, M., López Callejas, R., Gehr, R., Jiménez Cisneros, B.E., and Alvarez, P.J.J. (2001) *Water Res.*, **35**, 373–378.

121 Payne, K.B. and Abdel-Fattah, T.M. (2005) *J. Environ. Sci. Health, Part A*, **40**, 723–749.
122 Dousová, B., Grygar, T., Martaus, A., Fuitová, L., Kolousek, D., and Machovic, V. (2006) *J. Colloid Interface Sci.*, **302**, 424–431.
123 Xu, Y.-H., Nakajima, T., and Ohki, A. (2002) *J. Hazard. Mater.*, **92**, 275–287.
124 Tao, Y.S., Kanoh, H., Abrams, L., and Kaneko, K. (2006) *Chem. Rev.*, **106**, 896–910.
125 Davis, M.E. (2002) *Nature*, **417**, 813–821.
126 Drews, T.O. and Tsapatsis, M. (2005) *Curr. Opin. Colloid Interface Sci.*, **10**, 233–238.
127 Valdés, M.G., Pérez-Cordoves, A.I., and Díaz-García, M.E. (2006) *Trends Anal. Chem.*, **25**, 24–30.
128 Prasada Rao, T., Daniel, S., and Mary Gladis, J. (2004) *Trends Anal. Chem.*, **23**, 28–35.
129 Nishide, H. and Tsuchida, E. (1976) *Makromol. Chem.*, **177**, 2295–2310.
130 Nishide, H., Deguchi, J., and Tsuchida, E. (1976) *Chem. Lett.*, 169–174.
131 Bae, S.Y., Southard, G.L., and Murray, G.M. (1999) *Anal. Chim. Acta*, **397**, 173–181.
132 Shirvani-Arani, S., Ahmadi, S.J., Bahrami-Samani, A., and Ghannadi-Maragheh, M. (2008) *Anal. Chim. Acta*, **623**, 82–88.
133 Biju, V.M., Gladis, J.M., and Rao, T.P. (2003) *Anal. Chim. Acta*, **478**, 43–51.
134 Rosatzin, T., Andersson, L.I., Simon, W., and Mosbach, K. (1991) *J. Chem. Soc. Perkin Trans. 2*, 1261–1265.
135 Garcia, R., Pinel, C., Madic, C., and Lemaire, M. (1998) *Tetrahedron Lett.*, **39**, 8651–8654.
136 Rao, T.P., Kala, R., and Daniel, S. (2006) *Anal. Chim. Acta*, **578**, 105–116.

Edited by David T. Pierce and Julia Xiaojun Zhao

Trace Analysis with Nanomaterials

WILEY-VCH Verlag GmbH & Co. KGaA

The Editors

Dr. David T. Pierce
University of North Dakota
Department of Chemistry
151 Cornell Street, Stop 9024
Grand Forks, ND 58202-9024
USA

Dr. Julia Xiaojun Zhao
University of North Dakota
Department of Chemistry
151 Cornell Street, Stop 9024
Grand Forks, ND 58202-9024
USA

Library of Congress Card No.: applied for

British Library Cataloguing-in-Publication Data
A catalogue record for this book is available from the British Library.

Bibliographic information published by the Deutsche Nationalbibliothek
The Deutsche Nationalbibliothek lists this publication in the Deutsche Nationalbibliografie; detailed bibliographic data are available on the Internet at <http://dnb.d-nb.de>.

Composition Toppan Best-set Premedia Limited, Hong Kong

Printing and Bookbinding Strauss GmbH, Mörlenbach

Cover Design Adam Design, Weinheim

Printed in the Federal Republic of Germany
Printed on acid-free paper

ISBN: 978-3-527-32350-0